TU Delft

Delft University of Technology

Treadmilling by FtsZ filaments drives peptidoglycan synthesis and bacterial cell division

Bisson-Filho, Alexandre W.; Hsu, Yen Pang; Squyres, Georgia R.; Kuru, Erkin; Wu, Fabai; Jukes, Calum; Sun, Yingjie; Dekker, Cees; Holden, Seamus; VanNieuwenhze, Michael S.

DOI
10.1126/science.aak9973

Publication date
2017

Document Version
Final published version

Published in
Science

Citation (APA)
Bisson-Filho, A. W., Hsu, Y. P., Squyres, G. R., Kuru, E., Wu, F., Jukes, C., Sun, Y., Dekker, C., Holden, S., VanNieuwenhze, M. S., Brun, Y. V., & Garner, E. C. (2017). Treadmilling by FtsZ filaments drives peptidoglycan synthesis and bacterial cell division. *Science*, *355*(6326), 739-743. https://doi.org/10.1126/science.aak9973

Important note
To cite this publication, please use the final published version (if applicable).
Please check the document version above.

Copyright
Other than for strictly personal use, it is not permitted to download, forward or distribute the text or part of it, without the consent of the author(s) and/or copyright holder(s), unless the work is under an open content license such as Creative Commons.

Takedown policy
Please contact us and provide details if you believe this document breaches copyrights.
We will remove access to the work immediately and investigate your claim.

This work is downloaded from Delft University of Technology.
For technical reasons the number of authors shown on this cover page is limited to a maximum of 10.

Erratum 17 January 2020. See Erratum on pages 6-10.

REPORT

BACTERIAL DIVISION

Treadmilling by FtsZ filaments drives peptidoglycan synthesis and bacterial cell division

Alexandre W. Bisson-Filho,[1]‡ Yen-Pang Hsu,[2]‡ Georgia R. Squyres,[1]‡ Erkin Kuru,[2]*‡ Fabai Wu,[3]† Calum Jukes,[4] Yingjie Sun,[1] Cees Dekker,[3]§ Seamus Holden,[4]§ Michael S. VanNieuwenhze,[2,5]§ Yves V. Brun,[6]§ Ethan C. Garner[1]§

The mechanism by which bacteria divide is not well understood. Cell division is mediated by filaments of FtsZ and FtsA (FtsAZ) that recruit septal peptidoglycan-synthesizing enzymes to the division site. To understand how these components coordinate to divide cells, we visualized their movements relative to the dynamics of cell wall synthesis during cytokinesis. We found that the division septum was built at discrete sites that moved around the division plane. FtsAZ filaments treadmilled circumferentially around the division ring and drove the motions of the peptidoglycan-synthesizing enzymes. The FtsZ treadmilling rate controlled both the rate of peptidoglycan synthesis and cell division. Thus, FtsZ treadmilling guides the progressive insertion of new cell wall by building increasingly smaller concentric rings of peptidoglycan to divide the cell.

In most bacteria, cell division involves the inward synthesis of peptidoglycan (PG), creating a septum that cleaves the cell in two. The location of the septal PG synthases is regulated by filaments of the tubulin homolog FtsZ, which associate with the cytoplasmic side of the membrane via the actin-like FtsA and other factors. FtsZ forms membrane-associated filaments with FtsA (FtsAZ) (*1*, *2*). Together, they form a dynamic structure, the Z ring, which encircles the cell at the future division site (*3*) and recruits PG synthases and other proteins involved in cytokinesis (*4*). Once the division machinery is mature, the Z ring constricts while the associated synthases build the septum that partitions the cell in two.

We do not have a clear understanding of how the components of cell division interact in space and time to carry out cytokinesis, as we have been unable to observe the dynamics of each component relative to each other or to the structure they build: The organization and dynamics of FtsZ filaments within the Z ring remain ill-defined; it is not known how FtsAZ filaments control the activity of PG synthases; and the dynamics of septal PG synthesis have never been directly observed. To gain insight into how these components work together to divide bacteria, we visualized the dynamics of septal PG synthesis in

[1]Molecular and Cellular Biology, Faculty of Arts and Sciences Center for Systems Biology, Harvard University, Cambridge, MA 02138, USA. [2]Department of Molecular and Cellular Biochemistry, Indiana University, Bloomington, IN 47405, USA. [3]Department of Bionanoscience, Kavli Institute of Nanoscience Delft, Delft University of Technology, Netherlands. [4]Centre for Bacterial Cell Biology, Institute for Cell and Molecular Biosciences, Newcastle University, Newcastle upon Tyne NE2 4AX, UK. [5]Department of Chemistry, Indiana University, Bloomington, IN 47405, USA. [6]Department of Biology, Indiana University, Bloomington, IN 47405, USA.
*Present address: Department of Genetics, Harvard Medical School, Boston, MA 02115, USA. †Present address: Division of Geology and Planetary Sciences, California Institute of Technology, Pasadena, CA 91125, USA. ‡These authors contributed equally to this work. §Corresponding author. Email: egarner@g.harvard.edu (E.C.G.); mvannieu@indiana.edu (M.S.V.); ybrun@indiana.edu (Y.V.B.); seamus.holden@newcastle.ac.uk (S.H.); c.dekker@tudelft.nl (C.D.)

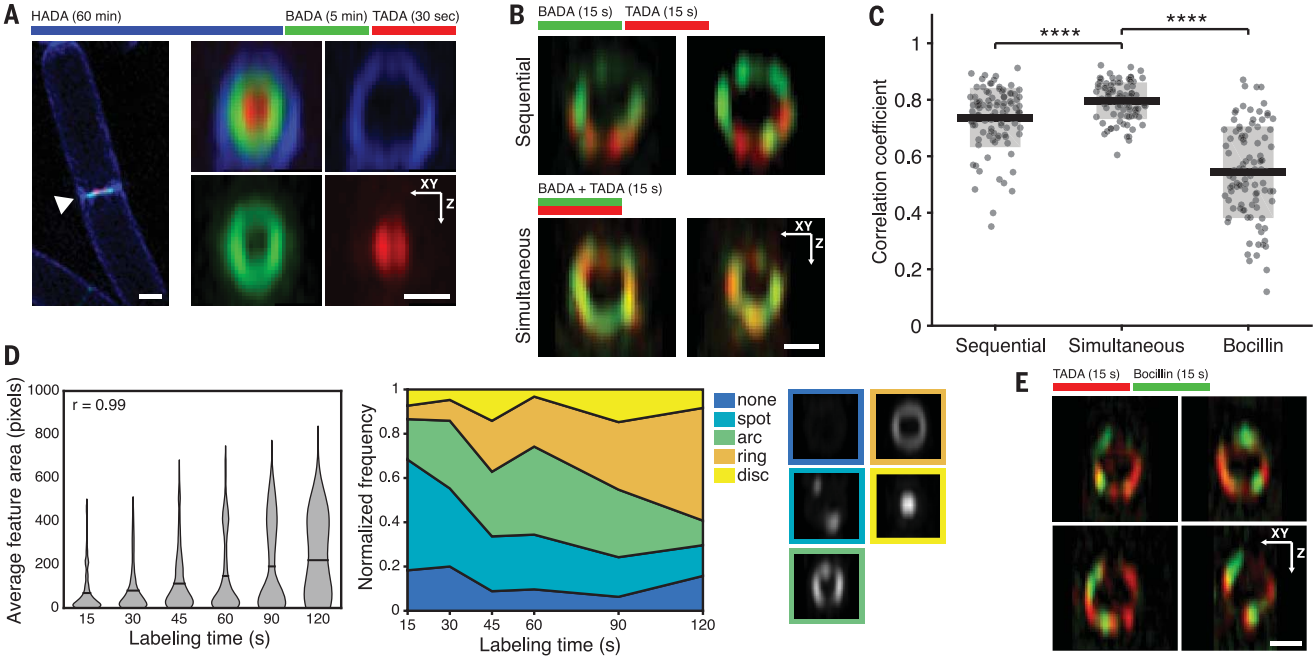

Fig. 1. Septal PG synthesis occurs at discrete, mobile sites. (**A**) Sequential FDAA labeling (HADA, 7-hydroxycoumarin-3-carboxylic acid–D-alanine; BADA, BODIPY FL-D-alanine; TADA, TAMRA–D-alanine) of division septa shows outside-in synthesis (arrowhead). (Right) 90° rotations of septa. (**B**) Sites of PG synthesis move around the septum. (**C**) Correlation coefficient of overlap between colors (yellow) in (B) and (E). Line, mean; box, SD. ****$P < 0.0001$. (**D**) FDAA labeling proceeds from puncta to complete rings. (Left) Area of FDAA features increases with pulse length. Lines, mean; *r*, correlation coefficient of the means. (Center) Blinded classification of FDAA features at various pulse lengths. (Right) Representative images of septal PG structures. (**E**) Sites of PG synthesis are offset from synthetic enzymes. Colored bars indicate time course of FDAA labeling. All images were taken with 3D-SIM. Scale bars, 0.5 μm.

Downloaded from http://science.sciencemag.org/ on October 26, 2020

Erratum 17 January 2020. See Erratum on pages 6-10.

relation to the movements of FtsAZ filaments and the septal PG synthase Pbp2B in the Gram-positive *Bacillus subtilis*.

To assess the dynamics of septal PG synthesis, we sequentially pulse-labeled growing cells with different colors of fluorescent D-amino acids (FDAAs) (table S1), which are incorporated into PG (*5*) by the D,D-transpeptidation activity of penicillin-binding proteins (PBPs) (*6*). Three-dimensional (3D)–structured illumination microscopy (3D-SIM) showed that sequential three-color FDAA pulse-labeling resulted in bull's-eye patterns at the division plane (Fig. 1A), demonstrating that the septum is progressively synthesized inward from the cell surface. Short, sequential pulses of two FDAA colors resulted in discrete spots or arcs distributed around the septum, with the colors more offset than for cells pulsed simultaneously (Fig. 1, B and C, and fig. S1, A and B). Thus, PG synthesis occurs at discrete sites that move around the division plane.

We next observed how discrete sites of PG synthesis develop into a complete division septum by labeling cells with FDAAs with increasing pulse durations. Both the total amount of labeling and the area of labeled regions increased with pulse duration (Fig. 1D, left, and fig. S2, A to C). Following short pulses, septa contained discrete spots or arcs (fig. S1C). As pulse duration increased, these arcs elongated and gradually transitioned into complete rings at longer pulses (Fig. 1D, right). As expected, PG synthesis inhibitors reduced FDAA incorporation (fig. S2D). To explore the location of the PG synthases relative to newly incorporated PG, we followed short FDAA pulses with Bocillin, which labels active PBPs (*7*) while inactivating them. The Bocillin signal was offset from the newly synthesized PG (Fig. 1, C and E), suggesting that the PG synthases also move around the division plane.

We next examined the motions of the division-specific PG synthases and their associated cytoskeletal polymers. Total internal reflection fluorescence microscopy (TIRFM) of a functional mNeonGreen-FtsZ fusion expressed from the native locus (fig. S3, A to E, and tables S2 and S3) revealed directional movements within newly assembled Z rings (Fig. 2A and movie S1).

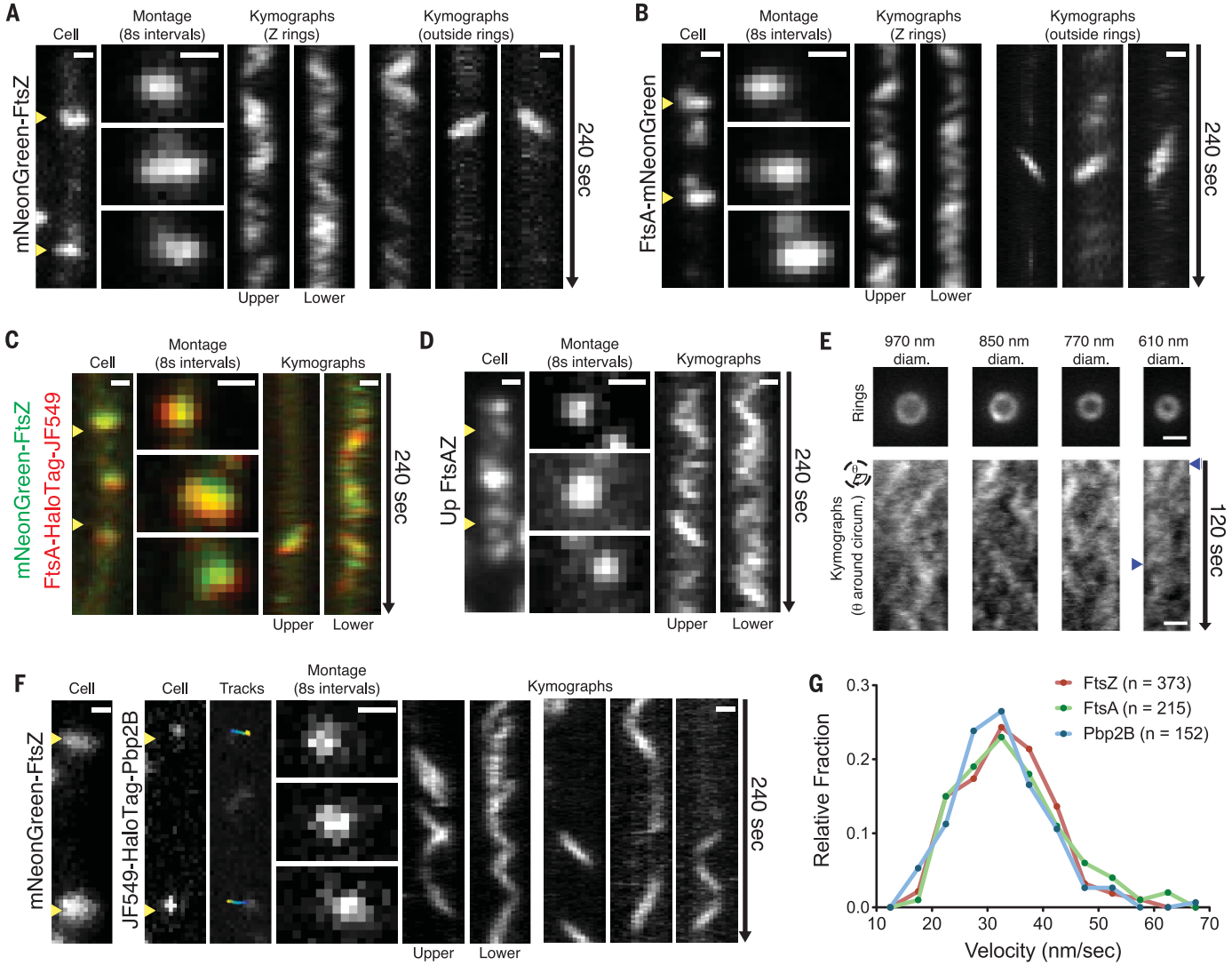

Fig. 2. FtsAZ and Pbp2B move directionally around the division site. (**A**) mNeonGreen-FtsZ (bAB185) shows directional motion inside (left) and outside (right) the Z ring; montage at 8-s intervals. (**B**) FtsA-mNeonGreen (bAB167) shows directional motion inside (left) and outside (right) the ring. (**C**) mNeonGreen-FtsZ and FtsA-HaloTag-JF549 (bAB229) colocalize and move together. Yellow is the overlap of green and red. (**D**) FtsAZ overexpression [100 μM isopropyl β-D-1-thiogalactopyranoside (IPTG) in bAB221] creates increased FtsZ filaments showing directional motion outside the Z ring. (**E**) Vertically immobilized cells (SH41) show multiple, independent mNeonGreen-FtsZ filaments moving in both directions around the division site. Cropped rings and radial kymographs in early (left), middle (center), and late (right) divisional stages. Blue arrowheads indicate directional FtsZ tracks. (**F**) Single molecules of Pbp2B (bGS31, 15-min incubation of 50 pM JF549) move directionally around the division site. Blue to yellow indicates trajectory time. Kymographs drawn at yellow arrowheads. Scale bars, 0.5 μm. (**G**) Velocity distributions of FtsA filaments, FtsZ filaments, and single Pbp2B molecules.

Downloaded from http://science.sciencemag.org/ on October 26, 2020

Erratum 17 January 2020. See Erratum on pages 6-10.

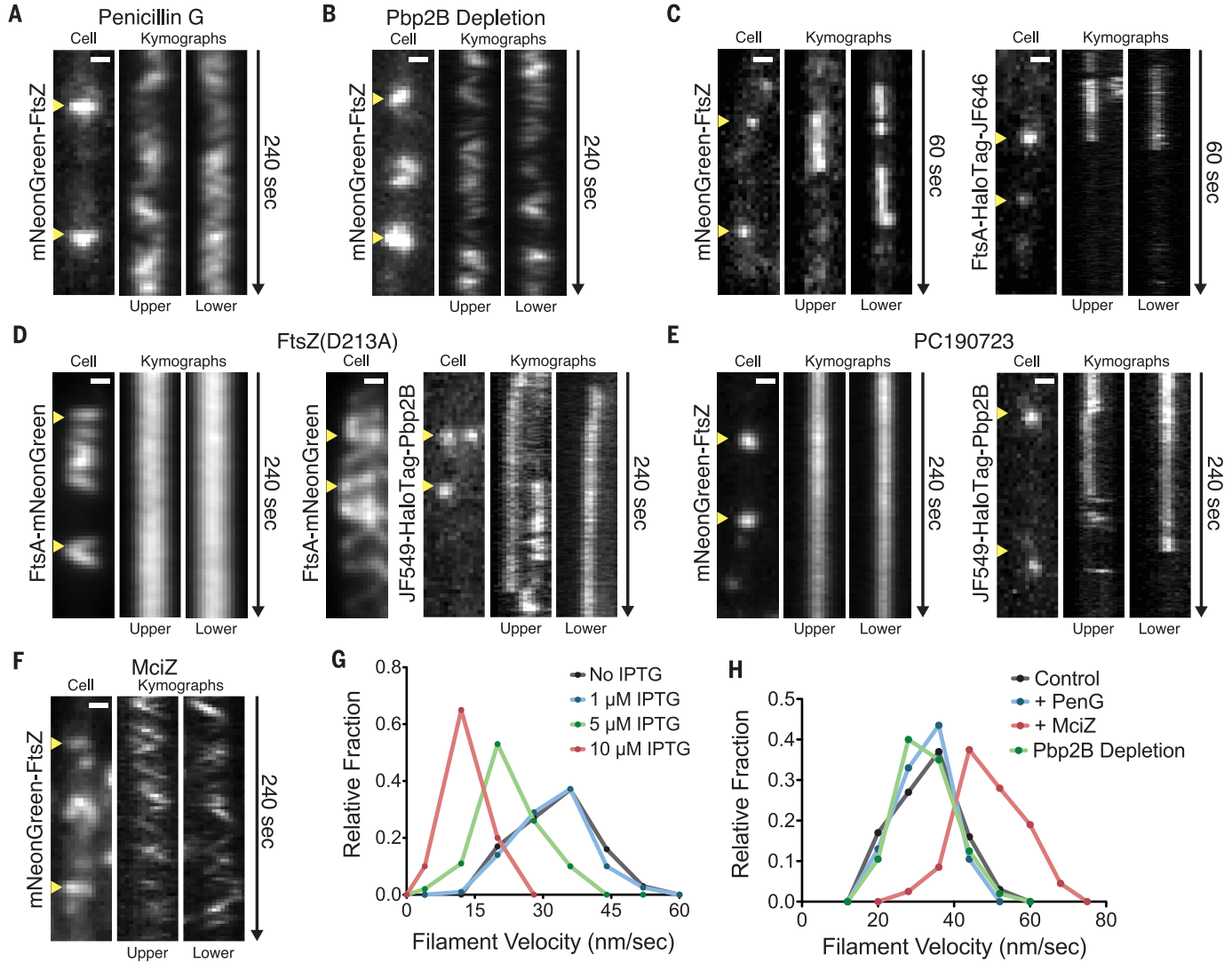

Fig. 3. Directional FtsAZ motion is driven by treadmilling, independent of cell wall synthesis, and is required for Pbp2B motion. (**A**) FtsZ continues to move directionally after treatment with penicillin G. bAB185 imaged 5 min after addition of 3 μl of 10 mg/ml penicillin G to an agarose pad. (**B**) FtsZ continues to move directionally after Pbp2B depletion. Before imaging, bGS31 was grown without IPTG until no divisions were observed (3 hours). (**C**) Single molecules of FtsZ and FtsA are immobile within the division site. Single molecules were obtained by growing bAB219 with no IPTG (left) or bAB229 with 15 min of 250 pM JF646 (right). (**D**) Overexpression of GTPase-deficient FtsZ stops FtsZ and Pbp2B motion. bAB217 (left) and bGS90 (right) were imaged after induction of FtsZ(D213A) (100 μM IPTG, 1 hour). (**E**) Directional motion of FtsZ and Pbp2B is stopped by PC190723. bAB185 (left) and bGS31 with 15-min incubation of 50 pM JF549 (right) 5 min after addition of 10 μM PC190723. (**F**) FtsZ velocity increases after exposure to MciZ. bAB185 was imaged after addition of 1 μM MciZ in a microfluidic device. Kymographs drawn at yellow arrowheads. Scale bars, 0.5 μm. (**G**) Velocity distributions of FtsZ filaments (bAB217) at different levels of FtsZ(D213A) induction. (**H**) Velocity distributions of FtsZ filaments under different perturbations.

Furthermore, in almost every cell, we observed small mNeonGreen-FtsZ filaments outside the Z ring moving directionally around the cell at the same rate as within Z rings, similar to oscillations previously observed in *Escherichia coli* (*8*). A functional FtsA-mNeonGreen fusion showed motions identical to FtsZ (Fig. 2B and movie S1), and two-color imaging confirmed that FtsA and FtsZ colocalized and moved together (Fig. 2C) (*9*). Overexpression of a second *ftsAZ* operon (FtsA, mNeonGreen-FtsZ) resulted in many more directionally moving filaments outside the Z ring that did not affect fitness (Fig. 2D and fig. S3F). To resolve FtsZ motion in dense, actively constricting Z rings, we vertically immobilized bacteria in agarose microholes, orienting the division plane parallel to the objective (fig. S4). This revealed multiple FtsZ filaments moving in both directions around the constriction site over a wide range of ring diameters (600 to 1000 nm) (Fig. 2E, fig. S4E, and movie S2). The movement of multiple FtsZ filaments around the Z ring may explain the heterogeneous structures and complex "patch" dynamics observed via superresolution microcopy (*10*–*12*), as well as the fast turnover of FtsZ subunits (*13*).

We next asked if the division-associated transpeptidase Pbp2B moves with FtsAZ. At native expression levels, mNeonGreen-Pbp2B moved directionally along the Z ring; this became more apparent with reduced expression (fig. S5, A and B). To observe the motions of single Pbp2B molecules, we labeled HaloTag-Pbp2B expressed from the native locus with low concentrations of HaloLigand-JF549 (*14*). TIRFM revealed two types of Pbp2B motion: (i) directional motion around the cell width, always localized to Z rings, and (ii) diffusion on the membrane, not localized to Z rings (Fig. 2F; fig. S5, C to E; and movie S3). We did not observe diffusive Pbp2B motion along Z rings at any acquisition rate. In some cases, we observed multiple Pbp2B molecules moving directionally within the same ring, sometimes in opposite directions, indicating that the Z ring contains multiple, independent synthetic

Downloaded from http://science.sciencemag.org/ on October 26, 2020

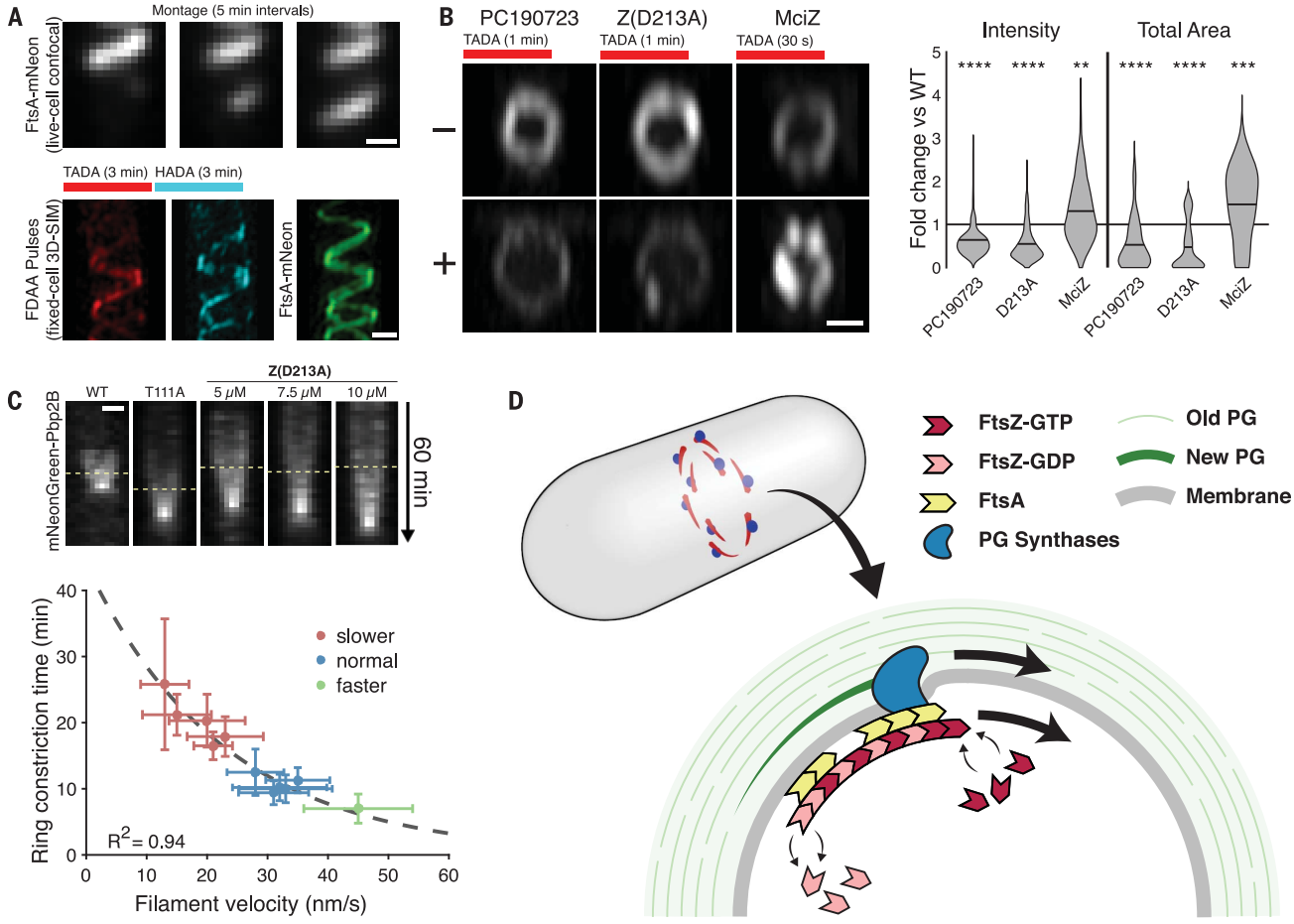

Fig. 4. Cytokinesis is controlled by directional motion of FtsAZ filaments. (**A**) FtsZ(D213A) overexpression (1 mM IPTG in bAB217) produces slowly growing FtsA spirals with spiral FDAA insertion. (Top) Montage of growing FtsA spiral acquired with spinning-disk confocal imaging. (Bottom) Sequential FDAA labeling and FtsA localization imaged with 3D-SIM in a fixed cell. (**B**) Altering FtsZ velocity changes the amount and total area of FDAA incorporation. (Left) PY79 with 1 μg/ml PC190723 for 10 min, (center) bAB217 with 20 μM IPTG for 1 hour, (right) AH93 with 50 mM xylose for 5 min. After treatment, cells were incubated with TADA for the indicated time, fixed, then imaged with 3D-SIM. (Far right) Total intensity and area of septal FDAA incorporation. Lines, mean. $^{**}P < 0.01$; $^{***}P < 0.001$; $^{****}P < 0.0001$. (**C**) Cytokinesis scales with FtsZ treadmilling velocity. For each condition, pairs of strains were used to measure (i) FtsZ velocity (using mNeonGreen-FtsZ) and (ii) septation rates (using mNeonGreen-Pbp2B). (Top) Kymographs of constricting Pbp2B rings in different FtsZ backgrounds (dashed line marks start of constriction). (Bottom) Plot of constriction time versus FtsZ velocity under different conditions. Treadmilling velocity and septation rates were acquired in identical conditions, save for measurements with MciZ (see supplementary materials). Error bars, SD of the mean. (A), (B), and (C): Scale bars, 0.5 μm. Dashed line in (C, bottom), slope. (**D**) Model for treadmilling-coupled cell division. (Top) The Z ring contains multiple FtsAZ filaments that treadmill around the division plane, pulling associated PG synthases. (Bottom) FtsZ treadmilling both regulates and distributes the activity of the PG synthases, building sequentially smaller uniform arcs of PG to divide the cell.

sites. FtsZ, FtsA, and Pbp2B all moved at similar velocities (Fig. 2G and fig. S5, D and E), suggesting that their motions are associated.

We investigated the mechanism driving FtsAZ/Pbp2B motion, first testing if, similar to MreB (*15*), Pbp2B inactivation would halt FtsAZ motion. However, FtsAZ motion was unaffected by multiple PG synthesis inhibitors (Fig. 3, A and H, and movie S4) or depletion of Pbp2B (Fig. 3, B and H, and movie S5).

We next tested if directional FtsAZ motion arose from filament treadmilling, as observed in vitro (*16*). Consistent with treadmilling, sparse labeling of FtsZ or FtsA in cells demonstrated that single molecules of both proteins were immobile within moving filaments (*17*) (Fig. 3C; fig. S5, F to J; and movie S6). Because treadmilling requires nucleotide hydrolysis, we assayed FtsA motion as we modulated the guanosine triphosphatase (GTPase) activity of FtsZ. Exogenous expression of FtsZ(D213A), a mutant shown to have greatly reduced GTPase activity in *E. coli* (*18*), gradually reduced FtsAZ velocity, stopping motion at high inductions (Fig. 3, D and G, and movie S7A). Likewise, addition of PC190723, an inhibitor of FtsZ guanosine triphosphate (GTP) hydrolysis (*19*) halted FtsZ movement (Fig. 3E and movie S8A). Conversely, addition of MciZ, a Z ring antagonist that, at low levels, increases FtsZ GTPase activity (*20*), increased FtsZ velocity (Fig. 3, F and H, and movie S7B). We next tested whether FtsZ treadmilling dynamics affected Pbp2B movement. PC190723 or overexpression of FtsZ(D213A) caused Pbp2B molecules to become immobile while the remaining colocalized with FtsZ (Fig. 3, D and E, and movie S8B). Pbp2B velocity scaled with FtsZ treadmilling velocity under various perturbations (fig. S5K). Thus, FtsZ treadmilling is required for the directional motions of both FtsAZ filaments and septal PG synthases.

Given the mobile nature of septal PG synthesis, we reasoned that the directional movements of FtsAZ and Pbp2B around the division plane could be coupled to septal PG synthesis. To test this, we labeled cells with FDAAs as we altered FtsZ dynamics. Overexpression of FtsZ(D213A) created long, slowly growing FtsA-mNeonGreen spirals, which incorporated FDAAs along their entire length (Fig. 4A and movie S9). Likewise, long PC190723 treatments resulted in fragmented patches of both FtsZ and FDAA incorporation (fig. S6A), indicating Pbp2B activity is constrained by FtsAZ location. However, these strong inhibitions of FtsZ dynamics required much longer pulses to achieve FDAA labeling, suggesting that FtsZ treadmilling limits PG synthesis. To test this, we

Downloaded from http://science.sciencemag.org/ on October 26, 2020

Erratum 17 January 2020. See Erratum on pages 6-10.

altered FtsAZ velocity as we pulse-labeled cells with FDAAs. This revealed that both the total amount and total area of PG synthesis within the ring are modulated by FtsAZ velocity: Conditions that slowed dynamics decreased both the total amount and area of FDAA labeling (Fig. 4B and fig. S6, B and C). Conversely, increasing FtsAZ velocity (with MciZ) increased both the total amount and area of labeling. Thus, in *B. subtilis*, both the amount and spatial distribution of septal PG synthesis are directly coupled to, and limited by, the rate of FtsZ filament treadmilling.

Because FtsAZ dynamics control the rate of septal synthesis, we asked whether the rate of cytokinesis depended on FtsAZ treadmilling. We modulated treadmilling velocity by (i) introducing mutations affecting GTP hydrolysis into FtsZ at the native locus, (ii) titrating exogenous FtsZ(D213A), (iii) expressing MciZ, and (iv) other perturbations (table S4). This revealed that the cytokinesis rate scaled with FtsZ treadmilling: Division was slower when velocity was decreased and faster when velocity was increased (Fig. 4C; fig. S7, A to C; and movie S10). Even under the strongest perturbations, these decreased rates of cytokinesis did not alter the rate of cell elongation (fig. S7, D to F). Thus, in *B. subtilis*, FtsAZ treadmilling is both coupled to, and limiting for, septal PG synthesis and cell constriction.

Our results indicate that cell division occurs by the action of discrete enzyme-filament complexes that, driven by FtsZ treadmilling, move around the division plane, building new PG during their transit (Fig. 4D). FtsZ treadmilling creates long-range order from the local activity of the PG synthases, linking circumferential enzyme motion to the insertion of cell wall. This tight coupling may yield uniform insertion of new material around the division plane, building the septum inward in progressively smaller concentric rings. Cell division slightly differs in *E. coli*, where FtsZ treadmilling also distributes PG synthesis around the ring (*21*), perhaps because the rate of PG synthesis is limiting relative to FtsZ treadmilling (*10*). This difference may arise from different levels of cell wall precursors between the two organisms or because *E. coli* must also couple PG synthesis to outer membrane insertion.

The coupling between FtsZ treadmilling and PG synthesis can unify previously conflicting models of cell division. FtsZ filaments have been proposed to generate force to bend membranes (*2*, *22*) and to scaffold PG synthesis (*10*, *23*). If FtsZ filaments deform membranes, coupling their movement to PG synthesis would allow each deformation to be reinforced by synthesis of PG (*24*). Thus, multiple sites of local deformation and coupled reinforcing synthesis moving around the division site would iteratively build the invaginating septum.

REFERENCES AND NOTES

1. Y. Chen, H. P. Erickson, *J. Biol. Chem.* **280**, 22549–22554 (2005).
2. P. Szwedziak, Q. Wang, T. A. M. Bharat, M. Tsim, J. Löwe, *eLife* **3**, e04601 (2014).
3. X. Ma, D. W. Ehrhardt, W. Margolin, *Proc. Natl. Acad. Sci. U.S.A.* **93**, 12998–13003 (1996).
4. P. Gamba, J. W. Veening, N. J. Saunders, L. W. Hamoen, R. A. Daniel, *J. Bacteriol.* **191**, 4186–4194 (2009).
5. E. Kuru *et al.*, *Angew. Chem. Int. Ed. Engl.* **51**, 12519–12523 (2012).
6. T. J. Lupoli *et al.*, *J. Am. Chem. Soc.* **133**, 10748–10751 (2011).
7. C. Eberhardt, L. Kuerschner, D. S. Weiss, *J. Bacteriol.* **185**, 3726–3734 (2003).
8. S. Thanedar, W. Margolin, *Curr. Biol.* **14**, 1167–1173 (2004).
9. V. W. Rowlett, W. Margolin, *Biophys. J.* **107**, L17–L20 (2014).
10. C. Coltharp, J. Buss, T. M. Plumer, J. Xiao, *Proc. Natl. Acad. Sci. U.S.A.* **113**, E1044–E1053 (2016).
11. S. J. Holden *et al.*, *Proc. Natl. Acad. Sci. U.S.A.* **111**, 4566–4571 (2014).
12. M. P. Strauss *et al.*, *PLOS Biol.* **10**, e1001389 (2012).
13. D. E. Anderson, F. J. Gueiros-Filho, H. P. Erickson, *J. Bacteriol.* **186**, 5775–5781 (2004).
14. J. B. Grimm *et al.*, *Nat. Methods* **12**, 244–250 (2015).
15. E. C. Garner *et al.*, *Science* **333**, 222–225 (2011).
16. M. Loose, T. J. Mitchison, *Nat. Cell Biol.* **16**, 38–46 (2014).
17. L. Niu, J. Yu, *Biophys. J.* **95**, 2009–2016 (2008).
18. S. D. Redick, J. Stricker, G. Briscoe, H. P. Erickson, *J. Bacteriol.* **187**, 2727–2736 (2005).
19. D. J. Haydon *et al.*, *Science* **321**, 1673–1675 (2008).
20. A. W. Bisson-Filho *et al.*, *Proc. Natl. Acad. Sci. U.S.A.* **112**, E2130–E2138 (2015).
21. X. Yang *et al.*, *bioRxiv* 10.1101/077610 (2016).
22. M. Osawa, H. P. Erickson, *Proc. Natl. Acad. Sci. U.S.A.* **110**, 11000–11004 (2013).
23. A. J. F. Egan, W. Vollmer, *Front. Microbiol.* **6**, 455 (2015).
24. Z. Li, M. J. Trimble, Y. V. Brun, G. J. Jensen, *EMBO J.* **26**, 4694–4708 (2007).

ACKNOWLEDGMENTS

We thank F. Gueiros-Filho, R. Losick, M. Erb, and P. Levin for strains; J. Xiao for discussions; L. Lavis for Janelia Fluor dyes; B. Murphy and E. Pasciak for FDAA synthesis help; F. Gueiros-Filho, R. Daniel, and J. Errington for antibodies; R. Losick, B. LaSarre, and D. Kearns for comments. This work was supported by NIH grants GM113172 to M.S.V. and Y.V.B., GM51986 to Y.V.B., and DP2AI117923-01 to E.C.G.; a Newcastle University Research Fellowship and Royal Society Research Grant RG150475 to S.H.; a Science Without Borders Research Fellowship to A.W.B.-F.; a European Research Council Advanced Grant (SynDiv 669598) to C.D.; and an NSF Graduate Research Fellowship Program (DGE1144152) to G.R.S. SIM was performed in the Indiana University Light Microscopy Imaging Center supported by S10RR028697-01. E.K., Y.V.B., and M.S.V. are inventors on U.S. Patent Application 14/395,815 (PCT Patent Application PCT/US2013/037504), submitted by the Indiana University Research and Technology Corporation, that covers the use of FDAAs for labeling of bacterial cell walls. Data are available in the text and supplementary materials. Movies S1 to S10 are also available at http://garnerlab.fas.harvard.edu/FtsZ/. Code is available at https://bitbucket.org/garnerlab/bisson-2016.

SUPPLEMENTARY MATERIALS

www.sciencemag.org/content/355/6326/739/suppl/DC1
Materials and Methods
Figs. S1 to S7
Tables S1 to S4
Movies S1 to S10
References (*25*–*45*)

26 September 2016; accepted 20 January 2017
10.1126/science.aak9973

Downloaded from http://science.sciencemag.org/ on October 26, 2020

Post date 17 January 2020

Erratum

In the Report "Treadmilling by FtsZ filaments drives peptidoglycan synthesis and bacterial cell division," the authors reported that a strain that expressed a sole copy of *ftsZ* fused to mNeonGreen (mNG) from the native locus [bAB185—*ftsA*-(*mNG-ftsZ*)]. Later, whole-genome sequencing revealed that this locus contained duplications of the *ftsAZ* operon (Fig. E1A). Likewise, the native locus fusions to *ftsA* revealed similar duplications (Fig. E1A).

To test if these duplications affected their measurements of filament dynamics or cell division rates, the authors created different merodiploid strains containing a second copy of the *ftsAZ* operon where each was labeled (Table E1). These mixed expression strains assembled competent Z-rings (Fig. E1B), as observed previously with both the duplicates and previously published merodiploid strains [AH175—*EYFP-ftsZ* in Handler *et al.* (*2*)—and SB168—(*ftsA-EGFP*)-*ftsZ* in Ben-Yehuda and Losick (*3*)]. All strains showed comparable distributions of cell lengths (Fig. E1C), a hallmark of cell division health; filament treadmilling rates (Fig. E1D); and cytokinesis periods (Fig. E1F).

To confirm the findings that (i) GTP hydrolysis drives FtsZ treadmilling and (ii) treadmilling limits cell division were not affected by these duplications, the authors measured how increasing the expression of FtsZ(D213A) altered the treadmilling rates and cytokinesis period with an independent FtsZ fusion from what was used in Bisson-Filho *et al.*, the previously published EYFP-FtsZ merodiploid (AH175). As before, increasing FtsZ(D213A) decreased treadmilling rates (Fig. E1E), while increasing the cytokinesis period (Fig. E1G). Overlaying their new measurements of treadmilling and constriction of all of these new tests onto the correlation plot in the original Fig. 4C of Bisson-Filho *et al.* indicated that all data fit into the previous trend (Fig. E1H). Thus, these additional measurements confirm that the strain duplications do not affect the Report's measurements or conclusions.

The authors additionally note that Fig. 2E from Bisson-Filho *et al.* shows FtsA-mNG dynamics rather than FtsZ-mNG as originally indicated, owing to an inadvertent error.

REFERENCES AND NOTES

1. A. W. Bisson-Filho *et al.*, Treadmilling by FtsZ filaments drives peptidoglycan synthesis and bacterial cell division. *Science*. **355**, 739–743 (2017).
2. A. A. Handler, J. E. Lim, R. Losick, Peptide inhibitor of cytokinesis during sporulation in Bacillus subtilis. *Mol. Microbiol.* **68**, 588–599 (2008).
3. S. Ben-Yehuda, R. Losick, Asymmetric cell division in B. subtilis involves a spiral-like intermediate of the cytokinetic protein FtsZ. *Cell*. **109**, 257–266 (2002).

Downloaded from http://science.sciencemag.org/ on October 26, 2020

10.1126/science.aba6311

Erratum 17 January 2020. See Erratum on pages 6-10.

Fig. E1. FtsZ treadmilling and cytokinesis are unperturbed despite the presence of multiple *ftsAZ* copies.

(**A**) Multiple copies of *ftsAZ* detected by Illumina and Nanopore whole-genome sequencing. Sequencing data from all strains, including the wild-type reference assembly, can be downloaded from https://garnerlab.fas.harvard.edu/BissonWGS.zip. (**B**) Comparison of Z-ring localization in different strains. Images were taken in both phase-contrast and FITC channels. (**C**) Box plots from cell length distributions from duplication and merodiploid strains. Cells were grown from single colonies to mid-exponential phase, diluted to an optical density at 600 nm (OD_{600}) of 0.05, and regrown to OD_{600} 0.5. Merodiploid strains were grown in the presence of 20 μM IPTG during the second growth cycle (~2.5 hours). Prior to imaging, cells were incubated with 1 μg/ml of FM5-95 (Invitrogen) membrane dye. (**D**) FtsAZ filament (and PBP2B single molecule) speeds present robust measurements across different strains despite the presence of the tagged divisome protein and fluorescent protein of choice. Strains used for measurements from Bisson-Filho *et al*. (2017) (left) and new data collected with different FtsAZ fusions from the literature (right). (**E**) FtsAZ treadmilling rates decrease under the expression of the FtsZ(D213A) mutant across multiple strains. (**F**) Cytokinesis periods are consistent across multiple strains using different fluorescent proteins tagging different components of the division machinery. (**G**) Cytokinesis periods consistently increase under the expression of the FtsZ(D213A) mutant across multiple strains. (**H**) Updated correlation plot as presented in Fig. 4C from Bisson-Filho *et al*. (2017) (black) with the new collected data (green) presented here. Correlation between cytokinesis and FtsZ treadmilling rates is unperturbed despite the presence of multiple *ftsAZ* copies, merodiploids, and fluorescent protein of choice

Downloaded from http://science.sciencemag.org/ on October 26, 2020

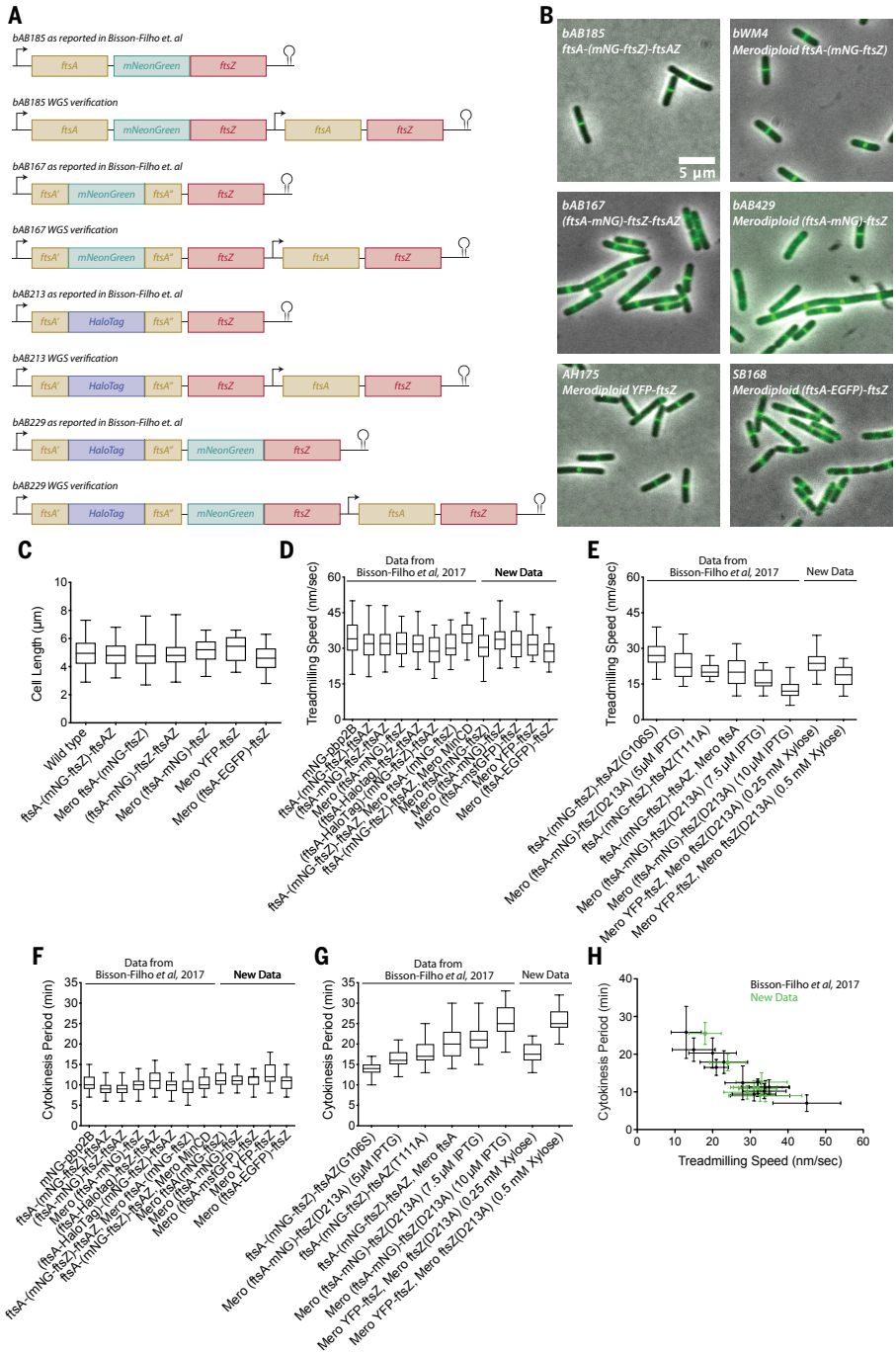

Downloaded from http://science.sciencemag.org/ on October 20, 2020

Erratum 17 January 2020. See Erratum on pages 6-10.

Table E1. Strains used in this study.

Strain	Description	Genotype	Reference
bWM4	mNG-FtsZ Merodiploid	*amyE::erm-Phyperspank-ftsA-mNeonGreen(M10S)-15aa(v2)-ftsZ(opt)*	This work
bAB431	FtsA-msfGFP Merodiploid	*amyE::erm-Phyperspank-ftsA-msfGFP(SW)-ftsZ*	Bisson-Filho *et al*. (2017)
bAB434	FtsA-msfGFP Complementation	*amyE::erm-Phyperspank-ftsA-msfGFP(SW)-ftsZ* *ftsAZ::cat-Pxyl-ftsAZ*	This work
bAB229	FtsA-HaloTag(SW)-mNG-ftsZ at the native site	*ftsAZ::erm-ftsA-HaloTag(SW)-mNeonGreen-15aa-ftsZ-cat*	Bisson-Filho *et al*. (2017)
bAB429	FtsA-mNG Merodiploid	*amyE::erm-Phyperspank-ftsA-Trunc_mNeonGreen(SW)-ftsZ*	This work
SB168	FtsA-GFP Merodiploid	*amyE::ftsAZ-cat::ftsA-gfp-ftsZ-kan*	Ben-Yehuda and Losick (2002)
bAB213	FtsA-HaloTag(SW) at the native site	*ftsA::erm-ftsA-HaloTag(SW)-cat*	Bisson-Filho *et al*. (2017)
AH175	YFP-FtsZ Merodiploid	*thrC::Pspac-YFP-ftsZ-erm*	Handler *et al*. (2008)
bAB185	mNG-FtsZ at the native site	*ftsZ::mNeonGreen-15aa-ftsZ*	Bisson-Filho *et al*. (2017)
bAB167	FtsA-mNeonGreen sandwich at the native site	*ftsA::ftsA-mNeonGreen(SW)*	Bisson-Filho *et al*. (2017)
bAB221	mNG-ftsZ at the native site mNG-FtsZ Merodiploid	*Native mNeonGreen-15aa-ftsZ* *amyE::erm-Physpank-ftsA-15aa-mNeonGreen-ftsZ*	Bisson-Filho *et al*. (2017)
bWM4	mNG-FtsZ Merodiploid	*amyE::erm-Phyperspank-ftsA-mNeonGreen(M10S)-15aa(v2)-ftsZ(opt)*	This work
bAB282	FtsZ-G106S (Z84) mutant at the native site FtsA-mNG-FtsZ under Physpank promoter	*amyE::erm-Physpank-ftsA-mNeonGreen-15aa-ftsZ* *ftsZ(G106S)-tetΩftsZ*	Bisson-Filho *et al*. (2017)
bAB281	FtsZ-T111A mutant at the native site FtsA-mNG-FtsZ under Physpank promoter	*amyE::erm-Physpank-ftsA-mNeonGreen-15aa-ftsZ* *ftsZ(T111A)-tetΩftsZ*	Bisson-Filho *et al*. (2017)
bAB199	mNG-ftsZ at the native site FtsA under Physpank promoter	*ftsZ::mNeonGreen-15aa-ftsZ* *amyE::erm-Physpank-ftsA*	Bisson-Filho *et al*. (2017)
bAB209	mNG-ftsZ at the native site MciZ under Pxyl promoter	*FtsZ::mNeonGreen-15aa-ftsZ* *amyE::Pxyl-mciZ-cat*	Bisson-Filho *et al*. (2017)
bAB248	mNG-ftsZ at the native site MinCD under Physpank promoter	*ftsZ::mNeonGreen-15aa-ftsZ* *amyE::Physpank-minCD-spc*	Bisson-Filho *et al*. (2017)
bAB217	FtsA-mNG and FtsZ-D213A mutant under Physpank promoter	*amyE::erm-Physpank-ftsA-mNeonGreen(SW)-ftsZ(D213A)*	Bisson-Filho *et al*. (2017)
ME7	Native mNG-Pbp2B	*pbpB::mNeonGreen-15aa-pbpB*	Bisson-Filho *et al*. (2017)
bAB156	YFP-FtsZ merodiploid FtsZ-D213A mutant under Pxyl promoter	*amyE::cat-Pxyl-ftsZ(D213A)* *thrC::Pspac-YFP-ftsZ-erm*	This work
bAB270	mNG-pbpB at the native site FtsZ-T111A mutant at the native site	*pbpB::mNeonGreen-15aa-pbpB* *ftsZ(T111A)-tetΩftsZ*	Bisson-Filho *et al*. (2017)

Downloaded from http://science.sciencemag.org/ on October 26, 2020

Erratum 17 January 2020. See Erratum on pages 6-10.

bAB271	mNG-pbpB at the native site ftsZ-G106S (Z84) mutant at the native site	*pbpB::mNeonGreen-15aa-pbpB ftsZ(G106S)-tetΩftsZ*	Bisson-Filho *et al*. (2017
bAB272	mNG-pbpB at the native site FtsAZ under Physpank promoter	*pbpB::mNeonGreen-15aa-pbpB amyE::erm-Physpank-ftsAZ*	Bisson-Filho *et al*. (2017)
bAB273	mNG-pbpB at the native site FtsA-mNG FtsZ-D213A mutant under Physpank promoter	*pbpB::mNeonGreen-15aa-pbpB amyE::erm-Physpank-ftsAZ(D213A)*	Bisson-Filho *et al*. (2017)
bAB274	mNG-pbpB at the native site MciZ under Pxyl promoter	*pbpB::mNeonGreen-15aa-pbpB amyE::cat-Pxyl-mciZ*	Bisson-Filho *et al*. (2017)
bAB285	mNG-pbpB at the native site MinCD under Physpabk promoter	*pbpB::mNeonGreen-15aa-pbpB amyE::Physpank-minCD-spc*	Bisson-Filho *et al*. (2017)
bAB153	ZapA-mNG at the native site	*zapA::zapA-40aa-mNeonGreen*	This work

Downloaded from http://science.sciencemag.org/ on October 26, 2020

Science

Treadmilling by FtsZ filaments drives peptidoglycan synthesis and bacterial cell division

Alexandre W. Bisson-Filho, Yen-Pang Hsu, Georgia R. Squyres, Erkin Kuru, Fabai Wu, Calum Jukes, Yingjie Sun, Cees Dekker, Seamus Holden, Michael S. VanNieuwenhze, Yves V. Brun and Ethan C. Garner

Science **355** (6326), 739-743.
DOI: 10.1126/science.aak9973

Coordinating cell wall synthesis and cell division

Most bacteria are protected by peptidoglycan cell walls, which must be remodeled to split the cell. Cell division requires the tubulin homolog FtsZ, a highly conserved cytoskeletal polymer that specifies the future site of division. Bisson-Filho *et al.* and Yang *et al.* found that the dynamic treadmilling of FtsZ filaments controls both the location and activity of the associated cell wall synthetic enzymes. This creates discrete sites of cell wall synthesis that circle around the division plane to divide the cell.

Science, this issue p. 739, p. 744

ARTICLE TOOLS http://science.sciencemag.org/content/355/6326/739

SUPPLEMENTARY MATERIALS http://science.sciencemag.org/content/suppl/2017/02/15/355.6326.739.DC1

RELATED CONTENT http://science.sciencemag.org/content/sci/355/6326/744.full
http://science.sciencemag.org/content/sci/367/6475/eaba6311.full

REFERENCES This article cites 42 articles, 18 of which you can access for free
http://science.sciencemag.org/content/355/6326/739#BIBL

PERMISSIONS http://www.sciencemag.org/help/reprints-and-permissions

Use of this article is subject to the Terms of Service

Science (print ISSN 0036-8075; online ISSN 1095-9203) is published by the American Association for the Advancement of Science, 1200 New York Avenue NW, Washington, DC 20005. The title *Science* is a registered trademark of AAAS.

Copyright © 2017, American Association for the Advancement of Science

Downloaded from http://science.sciencemag.org/ on October 26, 2020